ACS APPLIED MATERIALS & INTERFACES

Research Article

www.acsami.org

# A Facile Titanium Glycolate Precursor Route to Mesoporous Au/$Li_4Ti_5O_{12}$ Spheres for High-Rate Lithium-Ion Batteries

Cheng Chao Li,[†,‡] Qiu Hong Li,[†] Li Bao Chen,*[,†] and Tai Hong Wang*[,†]

[†]Key Laboratory for Micro-Nano Optoelectronic Devices of Ministry of Education and State Key Laboratory of Chemo/Biosensing and Chemometrics, Hunan University, Changsha, 410082, P. R. China

[‡]Department of Chemical and Biomolecular Engineering, National University of Singapore, 10 Kent Ridge Crescent, Singapore 119260

Supporting Information

**ABSTRACT:** A facile, green strategy is explored to synthesize mesoporous Au/$Li_4Ti_5O_{12}$ spheres based on in situ conversion of titanium glycolate in LiOH aqueous solution. Compared with $TiO_2$ precursors, titanium glycolate possesses some strengths: (i) fast and easy preparation; (ii) direct reaction with LiOH without introduce of $TiO_2$ impurity. In the synthesis, the produced chemical waste is only the mixed solvent of acetone and ethylene glycol (EG). Furthermore, acetone and EG in chemical waste can be easily separated by distillation and reused in the next synthesis process due to the great difference between their boiling points. In particular, the as-prepared mesoporous Au/$Li_4Ti_5O_{12}$ spheres combines the advantages of large specific surface area (166 $m^2/g$) and good electronic conduction enhanced by Au nanoparticles when used as an anode electrode material. The electrochemical tests show that the mesoporous Au/$Li_4Ti_5O_{12}$ spheres display excellent high rate capability and cycling performance.

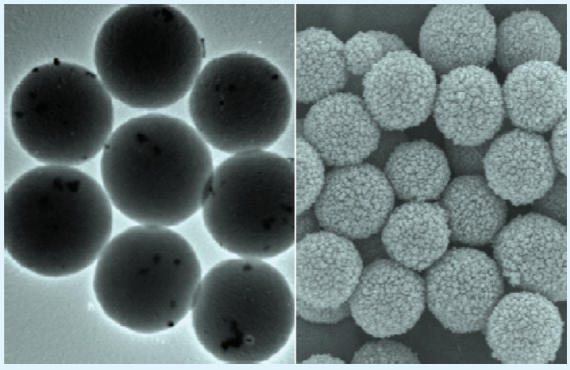

**KEYWORDS:** *mesoporous, spheres, lithium ion batteries, glycolate, lithium titanate, high-rate*

## INTRODUCTION

Lithium ion batteries have long been considered to be one of the most promising power sources for popular mobile devices, such as mobile phones, notebooks. Currently, most of the commercial lithium ion batteries have $LiCoO_2$ as a cathode and graphite as an anode.[1−3] However, the lithium-storage capacity of graphite especially in rate capability is not enough to meet the user's demand because of the continuous evolution of diversified multifeature devices with increasing power levels though they show good cycle behavior. The development of high-performance rechargeable lithium ion batteries for efficient energy storage has become one of the key components in today's information-rich mobile society. Current trend of research in rechargeable lithium ion battery technology is dedicated toward the development of lithium ion batteries, which have superior performance in terms of energy capacity, cycling stability, and rate capability.[4−6] This may be obtained only by achieving breakthroughs in electrode materials, as these devices depend intimately on the properties of their materials. To this end, a great deal of effort has been paid to the research and development of key materials.[7−10]

Spinel lithium titanate ($Li_4Ti_5O_{12}$) as a potential long-life anode material in high power lithium ion batteries as well as hybrid super capacitors has attracted great interest owing to its zero-strain characteristic during lithium insertion/extraction when compared with other anode materials.[11−16] The almost negligible volume change enables a stable cycle life. Besides, this active material shows a very flat potential plateau close to 1.55 V vs $Li^+/Li$, which is higher than the reduction potential of most organic electrolytes. The high discharge potential may stabilize the electrolytes and organic solvents since the reduction of electrolytes cannot occur at such a high potential. Despite these advantages, $Li_4Ti_5O_{12}$ still suffers from the problem of poor capacity at high rate because of its low electronic conductivity. Recent studies have demonstrated that use of nanosized or porous materials can improve the rate capability significantly because of their larger electrode−electrolyte contact area, shorter transport length for $Li^+$ and electronic transport. Unfortunately, the synthesis of nanosized or porous $Li_4Ti_5O_{12}$ material using conventional solid-state reactions or sol−gel routes is very difficult because these methods are carried out at high-temperature and cannot control the morphology, particle size and homogeneity, which have great effect on the electrochemical properties of the materials. Recently, several solution-based methods have been developed to synthesize porous $Li_4Ti_5O_{12}$ nanomaterials using $TiO_2$ as precursors.[17−20] The effective porous structure in a controllable fashion provides desirable surface area and open structure,

Received: September 30, 2011
Accepted: February 7, 2012
Published: February 7, 2012

   dx.doi.org/10.1021/am2018145 | ACS Appl. Mater. Interfaces 2012, 4, 1233−1238

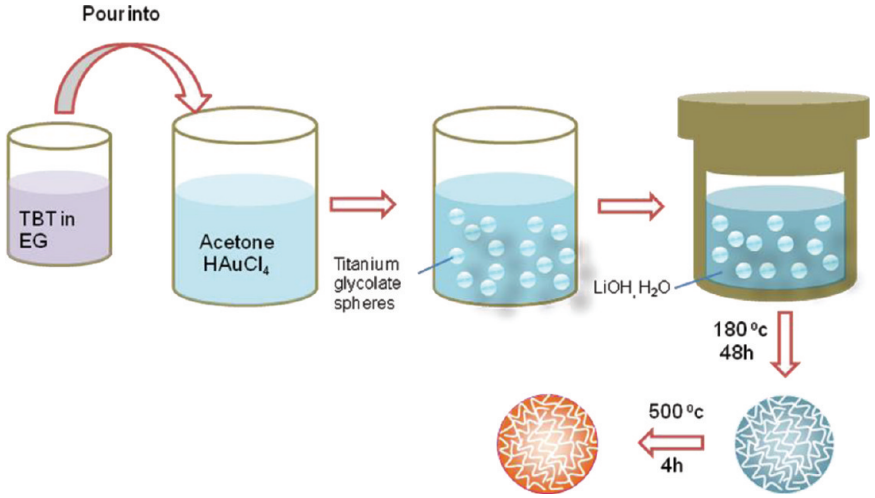


**Figure 1.** Schematic diagram for the preparation of the mesoporous Au/$Li_4Ti_5O_{12}$ spheres.

which can achieve higher rate capability and better cycle performance. However, $TiO_2$ impurity can be easily introduced into the products because of incomplete reaction.

Apart from reducing the dimension of materials, there is another route to improve the electrochemical performance, that is, introducing electronically conductive phases, such as carbon, carbon nanotubes, metal nanomaterials, polyacene, and so on.[21−24] The better electronic conduction can enhance the charge transfer of electrode materials, resulting high Li ion storage especially high-rate performance. For example, Huang et al. found that the incorporation of Ag clearly improved the rate capability and capacity retention due to the conductive effects of Ag nanoparticles.[23] Recently, Jiang group reported that the $Li_4Ti_5O_{12}$/carbon nanotubes composites exhibited better rate capability than those of pure $Li_4Ti_5O_{12}$.[24] They attributed the improved electrochemical performance to better electronic conduction of the nanocomposites.

Herein, we devise a facile, green strategy to synthesize mesoporous Au/$Li_4Ti_5O_{12}$ spheres by an in situ conversion route in water-isopropyl alcohol (IPA) mixed solution using titanium glycolate as a precursor. In comparison with $TiO_2$ precursors reported previously, titanium glycolate possesses many advantages: (i) fast and easy preparation; (ii) direct reaction with LiOH without introduce of $TiO_2$ impurity. The produced chemical waste in the synthesis is only the mixed solvent of acetone and EG, which can be easily separated by distillation and reused in the next synthesis process because of great difference between their boiling points. Importantly, the as-obtained mesoporous Au/$Li_4Ti_5O_{12}$ spheres possess a highly specific surface area of 166 $m^2/g$ and good conduction. As anode materials for high-rate lithium ion battery, the mesoporous Au/$Li_4Ti_5O_{12}$ spheres show excellent high-rate performance and capacity retention.

## EXPERIMENTAL SECTION

The schematic procedure for the preparation of mesoporous Au/$Li_4Ti_5O_{12}$ spheres is shown in Figure 1. The first step involved the preparation of the titanium glycolate precursor spheres adsorbed with $AuCl_4^-$. In the next step, the titanium glycolate spheres were converted into amorphous Au/$Li_4Ti_5O_{12}$ in the present of LiOH by hydrothermal reaction. Finally, the spinel Au/$Li_4Ti_5O_{12}$ spheres were obtained after calcinations. In this study, $HAuCl_4$ plays two important roles. First, $AuCl_4^-$ can adsorb on the surface of sphere and act as a stabilizing agent for the synthesis of monodisperse titanium glycolate spheres. Without the addition of $HAuCl_4$, the titanium glycolate spheres suffer from severe aggregation, as shown in Figure 2. On the other hand, $HAuCl_4$ can be reduced into Au nanoparticles in the reaction and act as an additive to improve the electrical conduction of $Li_4Ti_5O_{12}$ spheres, therefore improving the high rate capacity.

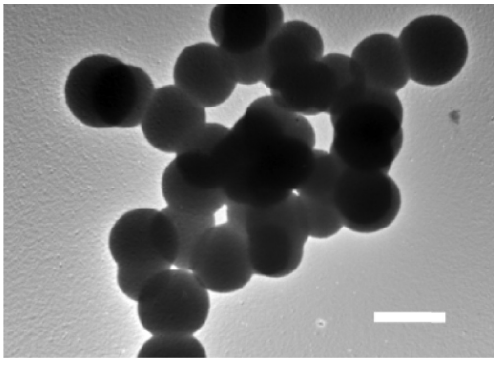

**Figure 2.** TEM images of titanium glycolate precursor prepared without addition of $HAuCl_4$. Scale bar: 500 nm.

**Synthesis of Titanium Glycolate Precursor Spheres.** The titanium glycolate precursor spheres were synthesized according to the route reported previously with minor modification.[25,26] In a typical synthesis, tetrabutoxytitanium (TBT, Aldrich) was added to ethylene glycol (EG, 50 mL; Merck) in a 100 mL flask under vigorous stirring; then the system was buddle with nitrogen for about 30 min to remove water and oxygen. After that, the flask was sealed and stirred for 8 h at room temperature. The obtained mixture was poured into 200 mL acetone in beaker, followed by addition of 1.9 mL of water and 0.8 mL of 30 mM $HAuCl_4$. The beaker was then sealed with parafilm and stirred for 1 h. The white precipitate was harvested by centrifugation and washing with ethanol for three times and dried at 50 °C in an oven for further usage.

**Synthesis of Mesoporous Au/$Li_4Ti_5O_{12}$ Spheres.** Fifty milligrams of titanium glycolate precursor was added to mixed solution of isopropyl alcohol and deionized water containing 1 mmol of LiOH under vigorous stirring. The mixture was transferred into a Teflon-lined autoclave with a volume of 50 mL and kept in an electric oven at 180 °C for 48 h. After being cooled down, the white product was collected by centrifugation and washed with deioned water and


dx.doi.org/10.1021/am2018145 | ACS Appl. Mater. Interfaces 2012, 4, 1233−1238

absolute ethanol several times, followed by drying in an oven at 80 °C for 12 h. Finally, the product was calcined at 500 °C for 4 h.

**Characterization.** Crystallographic phases of the prepared products were investigated by X-ray power diffraction method (XRD) using Shimadzu XRD-6000 with Cu K$\alpha$ radiation. The morphologies of the as-prepared sample were characterized by a field-emission scanning electron microscopy (FESEM; JSM-6700F), transmission electron microscopy (TEM; JEM-2010, 200 kV), selected area electron diffraction (SAED), and high-resolution transmission electron microscopy (HRTEM; JEM-3010, 300 kV). Fourier transform infrared (FTIR) spectrum was record for KBr dilute sample using a Bio-Rad FTS-135 FTIR spectrometer. Specific surface area measurement and porosity analysis for mesoporous $Li_4Ti_5O_{12}$ spheres samples were performed using $N_2$ adsorption−desorption isotherms (Quantachrome NOVA-3000 system at 77K). Au content was determined by inductively coupled plasma (ICP) emission spectroscopy (Dual-view Optima 5300 DV ICP-OES system).

**Electrochemical Characterization.** Electrochemical studies were characterized in CR2016-type coin cell with a multichannel current static system Arbin (Arbin Instruments BT 2000, USA). The electrode materials were prepared by mixing the active material with 10 wt % carbon black and 20 wt % binder (LA133 and CMC) in distilled water to form homogeneous slurry. The well-mixed slurry was then spread onto a copper foil and dried at 105 °C in a vacuum oven for 12 h. Circular disk electrodes were punched from the foil and a lithium metal foil was used as the counter electrode. One molar $LiPF_6$ in a mixture of ethylene carbonate (EC), dimethyl carbonate (DMC), and ethyl methyl carbonate (EMC) (EC:DC:DMC = 1:1:1) was used as the electrolyte. The assembly of the test cells was performed in an argon-filled glovebox using Li foil as counter electrode, polypropylene (PP) film (Celgard 2400) as separator, the cells were discharge and charged galvanostatically between 1.0 and 2.5 V at room temperature. 1C is defined as the amount of discharge current the battery delivers when discharged in one hour to the point of 100% depth of discharge (the current density herein is 120 mA $g^{-1}$).

## RESULTS AND DISCUSSION

The phase structure of the as-synthesized samples was characterized using power X-ray diffraction (XRD); a representative diffraction pattern is shown in Figure 3. All

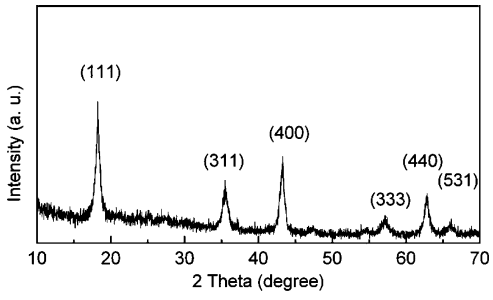


**Figure 3.** Powder XRD pattern of the mesoporous Au/$Li_4Ti_5O_{12}$ spheres.

these peaks can be indexed as spinel lithium titanate (space group $Fd\bar{3}m$, JCPDS card No. 49−0207).[27−29] The lattice parameter $a$ was found to be 0.837 nm by analysis of the X-ray pattern, which is in agreement with bulk cubic materials. The broadening of the diffraction peaks is ascribed to nanoscale structure of the material. No other peaks such as $TiO_2$ were detected, indicating the purity of the product.

Uniform-sized titanium glycolate spheres are synthesized in large scale using tetrabutoxytitanium and ethylene glycol (EG) as precursors. This experiment is based on a simple sol−gel route. The morphology of the precursor titanium glycolate spheres were investigated by scanning electron microscopy (SEM) and transmission electron microscopy (TEM). Figure 4

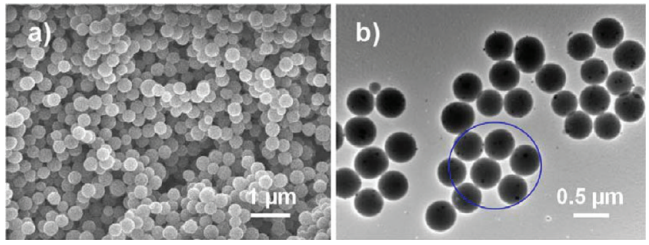


**Figure 4.** Representative (a) SEM and (b) TEM images of the as-prepared titanium glycolate spheres.

shows the representative SEM and TEM images of the as-prepared titanium glycolate spheres. From Figure 4a, we found that the product consisted of monodispersed spheres with sizes of 400−500 nm. TEM image (Figure 4b) shows that the titanium glycolate spheres have uniform size and rather smooth surface. Some Au nanoparticles were clearly observed on the surface of these spheres. We speculated the $AuCl^{4-}$ adsorbed on the spheres were partly reduced by EG with the assistance of ultrasonication. The content of gold detected by inductively coupled plasma (ICP) is around 0.9%. The chemical composition and bonding situation of the spheres have been investigated by FTIR (Figure 5). The band at around 3340 $cm^{-1}$

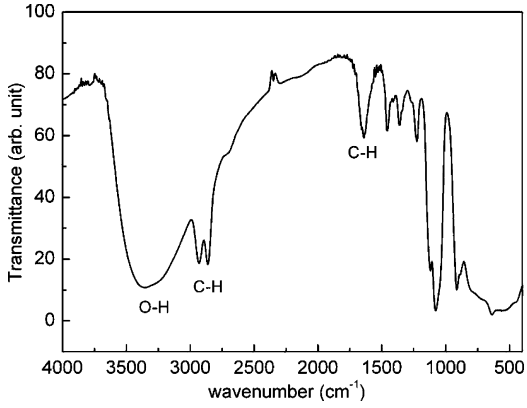


**Figure 5.** Representative FTIR spectrum of as-prepared titanium glycolate spheres.

assigned to the stretching mode of O−H group; the peaks at 2930, 2865, and 1635 $cm^{-1}$ corresponding to the C−H, which is clear evidence of the existence of EG.[25,26] After the hydrothermal reaction between titanium glycolate and LiOH at 180 °C, SEM images of the product reveals that the size and spherical morphologies can be completely preserved. The TEM images also confirmed porous nature of the materials, as shown in Figure 6a. The pores in mesoporous spheres (about several nanometers) are clearly observed. The mesoporous spheres consist of a lot of interconnected nanoparticles of ca. 10 nm size. The High resolution TEM (HRTEM) image (Figure 6d) shows clear lattice fringes with an interfringe distance of approximately 0.48 nm, which corresponds to the lattice spacing of the {111} planes. To investigate the porous structure of the as-obtained $Li_4Ti_5O_{12}$ spheres, we have carried out nitrogen adsorption/desorption measurements at 77 K. Figure 7 presents the isotherm of the


dx.doi.org/10.1021/am2018145 | ACS Appl. Mater. Interfaces 2012, 4, 1233−1238

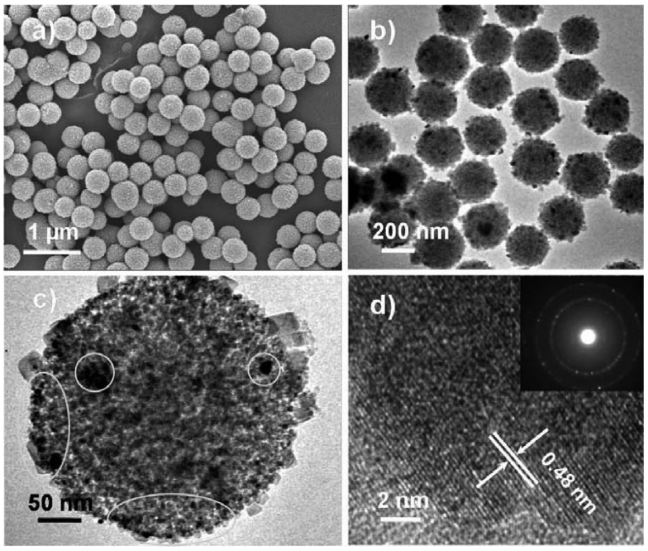


**Figure 6.** Typical (a) SEM, (b, c) TEM, and (d) HRTEM images of the mesoporous Au/$Li_4Ti_5O_{12}$ spheres.

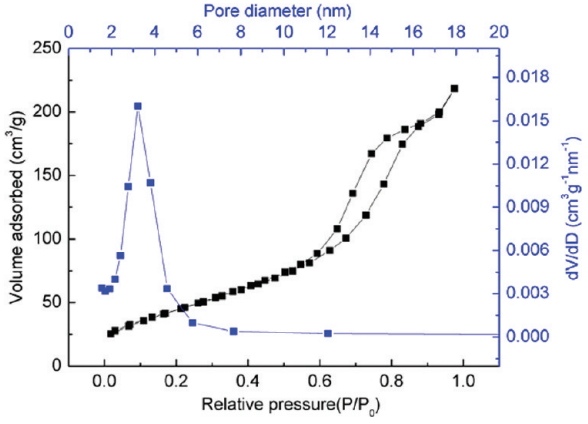


**Figure 7.** $N_2$ adsorption−desorption BET isotherm and pore size distribution curve.

$Li_4Ti_5O_{12}$ spheres and its corresponding pore size distribution curve. The isotherm can be classified as a type IV isotherm characteristic of mesoporous materials. The corresponding pore size distribution calculated from the isotherm by the Barrett−Joyner−Halenda (BJH) method shows a narrow pore size distribution ranging from 2 to 5 nm. The Brunauer−Emmett−Teller (BET) surface area and pore volume are 166 $m^2/g$ and 0.32 $m^3/g$, respectively. Most importantly, major chemicals (acetone and EG) in this work can be easily recovered by distillation at 80 °C due to the great difference in the boiling point (EG, bp: 197.8 °C, acetone bp: 56 °C). Gas chromatograph (GC) results indicated that used acetone can be completely separated from product remains with a purity of ~99% (see Figure SI-1 in the Supporting Information). Besides, the recycled acetone was used again to prepare titanium glycolate spheres; no difference can be found by using fresh acetone or recycled one (seeFigure SI-2 in the Supporting Information).

On the basis of experimental results, the mesoporous sphere formation of Au/$Li_4Ti_5O_{12}$ can be explained by a localized kirkendall effect. The main reaction in the solution is the liquid−solid interface reaction between the LiOH and titanium glycolate precursor. Herein, titanium glycolate spheres act as both site template and reactant. After titanium glycolate spheres were added to the IPA-water solution containing LiOH, LiOH and $H_2O$ would first react with titanium glycolate on the surface of spheres to form porous amorphous $Li_4Ti_5O_{12}$ shell. Then, LiOH and $H_2O$ would enter into the spheres and interact with titanium glycolate to form amorphous $Li_4Ti_5O_{12}$. The outer shells, acting as buffer layer, not only protect the sphere from cracking, but also prevent the fast outward diffusion of titanium species. Without the protection of the outer shells, the produced titanium hydroxyl species would quickly diffuse to the outer solution and nucleate. On the other hand, the inward diffusion rate of water is much faster than the outward diffusion of titanium species. Therefore, the reaction is localized inside spheres, and porous structure was achieved. It should be noted that mesoporous spheres can hardly be obtained from titanium glycolate precursors obtained by low concentration TBT. The obtained titanium glycolate precursors are also monodisperse spheres without any difference with the typical procedure, as shown in Figure 8. During the process of hydrolysis, relatively high concentration of $OH^-$ led the fast diffusion of titanium hydroxyl species through the shells, resulting outside growth. Figure 9 shows the TEM images of $Li_4Ti_5O_{12}$ using titanium glycolate spheres precursors with different TBT concentration ((a) 0.8 mL of TBT in 50 mL of EG; (b) 1.5 mL of TBT in 50 mL of EG). From the images, a lot of sheetlike structure can be found in the products. Therefore, for in situ conversion synthesis of nanostructures, one must carefully control nucleation kinetics by reactant concentrations because good morphology preservation becomes favorable in a conversion process with suitable reaction rate.

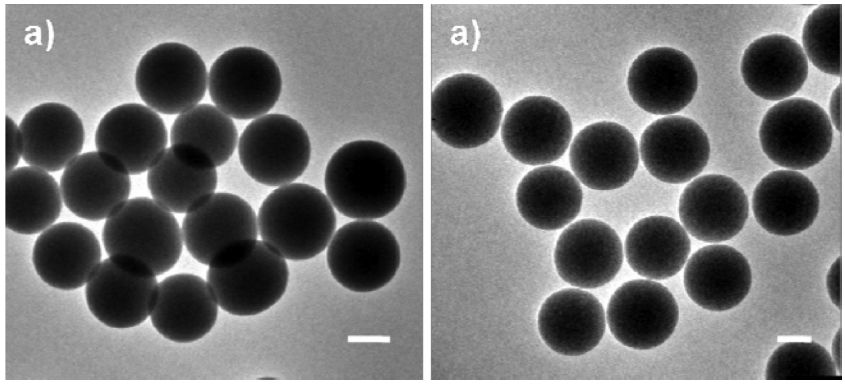


**Figure 8.** Representative TEM images of titanium glycolate spheres prepared at low TBT concentration: (a) 0.8 mL of TBT in 50 mL of EG, (b) 1.5 mL of TBT in 50 mL of EG.

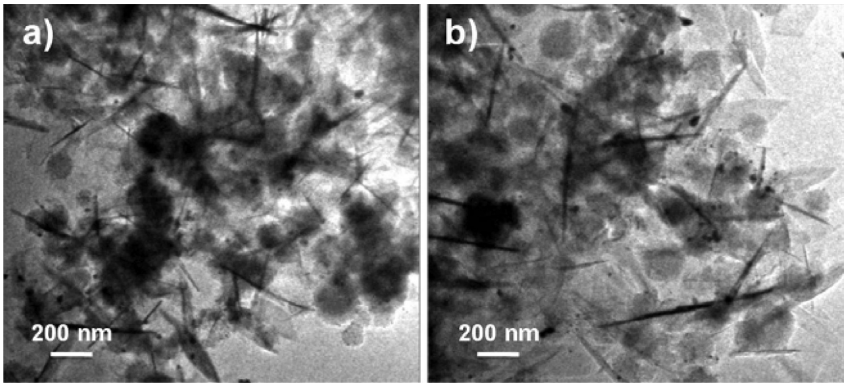


**Figure 9.** TEM images of $Li_4Ti_5O_{12}$ obtained by titanium glycolate spheres precursors with different TBT concentration ((a) 0.8 mL of TBT in 50 mL of EG; (b) 1.5 mL of TBT in 50 mL of EG).

It has been suggested that good electronic conduction and large specific surface area are very important factors to enhance the electrochemical performance of Li-ion battery anodes. Intrigued by this interest, the mesoporous $Au/Li_4Ti_5O_{12}$ spheres were expected to be advantageous to high-rate performance lithium ion batteries because of their porous structure and enhanced electronic conduction by Au nanoparticles. Figure 10a depicts the first charge/discharge curves of the mesoporous $Au/Li_4Ti_5O_{12}$ spheres at different discharge current densities from 1C to 20C. The charge−discharge curves at a current density of 1C display a very flat charge/discharge plateau in the voltage range between 1.5 and 1.6 V, which is the reversible redox potential of spinel $Li_4Ti_5O_{12}$, and the discharge capacity reaches 164 mA h $g^{-1}$ to an end voltage of 1.0 V.[30] With increasing of the charge−discharge rates, the cell voltages decreased from 1.57 V at 1C to around 1.45 V at 20C, which is related to the sluggish diffusion kinetics of Li-ion at high rates. The corresponding rate performance was shown in Figure 10b. For each stage, the process was taken with 50 cycles. A specific discharge capacity is around 154.8 mA h $g^{-1}$ obtained at a rate of 1C. The specific discharge capacity was slightly reduced to 145, 135, and 127 $mAhg^{-1}$ at rates of 2C, 5C, and 10C, respectively. At the high rate of 20C, the specific charge capacity is still 120 mA h $g^{-1}$. It is clearly observed that the rate performance is much higher than that of plain $Li_4Ti_5O_{12}$ spheres (Figure 10b). Furthermore, the mesoporous $Au/Li_4Ti_5O_{12}$ spheres show much better high-rate performance compared to the $Li_4Ti_5O_{12}$ nanorods, $Li_4Ti_5O_{12}$ nanotubes, $Li_4Ti_5O_{12}$ nanowires, and $Li_4Ti_5O_{12}$ nanoparticles reported previously.[13a,27,28,31] The improved high-rate performance may be that attributed to the enhancement of electronic conductivity of Au nanoparticles and porous structures. Besides, the nanosized particles would definitely increase the efficiency of lithiation and delithiation, and are more capable of accommodating volume expansion. In particular, these rich and hierarchical diffusion channels facilitate electrolyte transportation and lithium ion diffusion, which ensure enough lithium ions to rapidly contact the much larger surfaces of the electro-active $Li_4Ti_5O_{12}$ spheres. To further investigate the cycling performance of mesporous $Li_4Ti_5O_{12}$ spheres, we charged/discharged the cell for 100 cycles at 0.5C and 1C, as shown in Figure 10c. The sample shows very high capacity retention. The discharge capacities in the first cycle was 175.0 and 154.1 mA h $g^{-1}$, after 100 cycles, the capacities still remained at 158.3 and 149.2 mA h $g^{-1}$ at 0.5C and 1C,

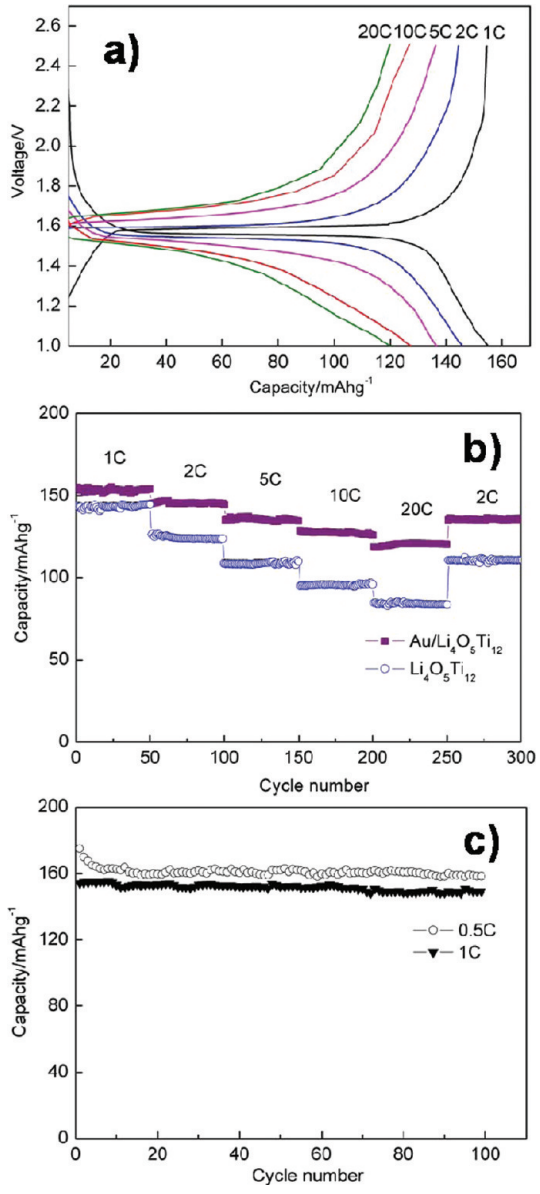


**Figure 10.** (a) First charge and discharge curves for the mesoporous $Au/Li_4Ti_5O_{12}$ spheres between 1.0 and 2.5 V at different current densities, (b) rate performance of the mesoporous $Au/Li_4Ti_5O_{12}$ spheres, (c) cycle performance of the mesoporous $Au/Li_4Ti_5O_{12}$ spheres at a current rate of 1C between 1.0 and 2.5 V.


dx.doi.org/10.1021/am2018145 | ACS Appl. Mater. Interfaces 2012, 4, 1233−1238

respectively. Although the capacities decrease in the initial several cycles, the total capacity fade only is around 2.5% during the 10−100th cycles. The excellent cycling ability can be ascribed to the nanosized particles, good crystallinity, and zero-volume expansion of mesporous $Li_4Ti_5O_{12}$ spheres over the whole stoichiometric range.

## CONCLUSIONS

We developed an in situ conversion route to synthesize mesoporous Au/$Li_4Ti_5O_{12}$ spheres in water-IPA mixed solution using titanium glycolate spheres as precursor. In the synthesis, the titanium glycolate spheres acted as both site template and reactant. Because of the large specific surface area and improved electronic conductivity by Au nanoparticles coating, the mesoporous Au/$Li_4Ti_5O_{12}$ spheres manifested superior high-rate performance and capacity retention when used as anode materials for lithium ion battery.

## ASSOCIATED CONTENT

### Supporting Information

TEM images and GC analysis report of recycled acetone. This material is available free of charge via the Internet at http://pubs.acs.org.

## AUTHOR INFORMATION

### Corresponding Author

*Tel: +86-0731-88823407. Fax: +86-0731-88822137. E-mail: lbchen@hnu.edu.cn (L.B.C.); thwang@iphy.ac.cn (T.H.W.).

### Notes

The authors declare no competing financial interest.

## ACKNOWLEDGMENTS

This work was partly supported from Scholarship Award for Excellent Doctoral Student granted by Ministry of Education (2010), "973" National Key Basic Research Program of China (Grant 2007CB310500), Chinese Ministry of Education (Grant 705040), and National Natural Science Foundation of China (Grant 90606009).

## REFERENCES

(1) Park, M. S.; Wang, G. X.; Kang, Y. M.; Wexler, D.; Dou, S. X.; Liu, H. K. *Angew. Chem., Int. Ed.* **2007**, *46*, 750.
(2) (a) Chen, J. S.; Tan, Y. L; Li, C. M.; Cheah, Y. L.; Luan, D.; Madhavi, S.; Boey, F. Y. C.; Archer, L. A.; Lou, X. W. *J. Am. Chem. Soc.* **2010**, *132*, 6124. (b) Lou, X. W.; Chen, J. S.; Chen, P.; Archer, L. A. *Chem. Mater.* **2009**, *21*, 2868. (c) Chen, J. S.; Zhu, T.; Yang, X. H.; Yang, H. G.; Lou, X. W. *J. Am. Chem. Soc.* **2010**, *132*, 13162.
(3) Chen, J.; Xu, L.; Li, W. Y.; Gou, X. L. *Adv. Mater.* **2005**, *17*, 582.
(4) (a) Kim, D. W.; Hwang, I. S.; Kwon, S. J.; Kang, H. Y.; Park, K. S.; Choi, Y. J.; Choi, K. J.; Park, J. G. *Nano Lett.* **2007**, *7*, 3041. (b) Chen, Y. J.; Zhu, C. L.; Xue, X. Y.; Shi, X. L.; Cao, M. S. *Appl. Phys. Lett.* **2008**, *92*, 223101. (c) Xue, X. Y.; Yuan, S.; Xing, L. L.; Chen, Z. H.; He, B.; Chen, Y. J. *Chem. Commun.* **2011**, *47*, 4718. (d) Xue, X. Y.; Chen, Z. H.; Xing, L. L.; Yuan, S.; Chen, Y. J. *Chem. Commun.* **2011**, *47*, 5205.
(5) Yu, Y.; Chen, C. H.; Shi, Y. *Adv. Mater.* **2007**, *19*, 993.
(6) Li, Y. G.; Tan, B.; Wu, Y. Y. *Nano Lett.* **2008**, *8*, 265.
(7) Wang, Y.; Xia, H.; Lu, L.; Lin, J. Y. *ACS Nano* **2010**, *4*, 1425.
(8) Zhan, F. M.; Geng, B. Y.; Guo, Y. J. *Chem.—Eur. J.* **2009**, *15*, 6169.
(9) (a) Li, C. C.; Yin, X. M.; Chen, L. B.; Li, Q. H.; Wang, T. H. *Chem.—Eur. J.* **2010**, *16*, 5215. (b) Li, C. C.; Yin, X. M.; Chen, L. B.; Li, Q. H.; Wang, T. H. *Appl. Phys. Lett.* **2010**, *97*, 043501. (d) Li, C. C.; Yin, X. M.; Chen, L. B.; Li, Q. H.; Wang, T. H. *J. Phys. Chem. C* **2010**, *113*, 13438.
(10) Ng, S. H.; Wang, J. Z.; Wexler, D.; Konstantinov, K.; Guo, Z. P.; Liu, H. K. *Angew. Chem., Int. Ed.* **2006**, *45*, 6896.
(11) (a) Ouyang, C. Y.; Zhong, Z. Y.; Lei, M. S. *Electrochem. Commun.* **2007**, *9*, 1107. (b) Yu, S. H.; Pucci, A.; Herntrich, T.; Willinger, M. G.; Baek, S. H.; Sung, Y. E.; Pinna, N. *J. Mater. Chem.* **2011**, *21*, 806. (c) Prakash, A. S.; Manikandan, P.; Ramesha, K.; Sathiya, M.; Tarascon, J. M.; Shukla, A. K. *Chem. Mater.* **2010**, *22*, 2837.
(12) (a) Li, J.; Tang, Z.; Zhang, Z. *Electrochem. Commun.* **2005**, *7*, 894. (b) Wang, Y. G.; Liu, H. M.; Wang, K. X.; Eiji, H.; Wang, Y. R.; Zhou, H. S. *J. Mater. Chem.* **2009**, *19*, 6789. (c) Park, K. S.; Benayad, A.; Kang, D. J.; Doo, S. G. *J. Am. Chem. Soc.* **2008**, *130*, 14930.
(13) (a) Jiang, C.; Ichihara, M.; Honma, I.; Zhou, H. S. *Electrochim. Acta* **2007**, *52*, 6470. (b) Zhang, B. H.; Yu, X. Y.; Ge, C. Y.; Dong, X. M.; Fang, Y. P.; Li, Z. S.; Wang, H. Q. *Chem. Commun.* **2010**, *46*, 9188. (c) Hirayama, M.; Kim, K.; Toujigamori, T.; cho, W.; Kanno, R. *Dalton. Trans.* **2011**, *40*, 2882. (d) Shen, L. F.; Yuan, C. Z.; Luo, H. J.; Zhang, X. G.; Xu, K.; Zhang, F. *J. Mater. Chem.* **2011**, *21*, 761.
(14) (a) Ge, H.; Li, N.; Li, D. Y.; Dai, C. S.; Wang, D. L. *Electrochem. Commun.* **2008**, *10*, 719. (b) Cheng, L.; Yan, J.; Zhu, G. N.; Luo, J. Y.; Wang, C. X.; Xia, Y. Y. *J. Mater. Chem.* **2010**, *20*, 595.
(15) Shenouda, A. Y.; Murali, K. *J. Power Sources* **2008**, *176*, 332.
(16) Wagemaker, M.; W. Borghols, J. H.; Mulder, F. M. *J. Am. Chem. Soc.* **2007**, *129*, 4323.
(17) Wang, D.; Xu, H. Y.; Gu, M.; Chen, C. H. *Electrochem. Commun.* **2009**, *11*, 50.
(18) Hsiao, K. C.; Liao, S. C.; Chen, J. M. *Electrochim. Acta* **2008**, *53*, 7242.
(19) Kim, D. H.; Ahn, Y. S.; Kim, J. *Electrochem. Commun.* **2005**, *7*, 1340.
(20) Tang, F.; Yang, L.; Qiu, Z.; Huang, J. S. *Electrochem. Commun.* **2008**, *10*, 1513.
(21) Gao, J.; Ying, J.; Jiang, C.; Wan, C. *J. Power Sources* **2007**, *166*, 255.
(22) Yu, H. Y.; Zhang, X. F.; Jalbout, A. F.; Yan, X. D.; Pan, X. M.; Xie, H. M.; Wang, R. S. *Electrochim. Acta* **2008**, *53*, 4200.
(23) Huang, S. H.; Wen, Z. Y.; Zhang, J. C.; Yang, X. L. *Electrochim. Acta* **2007**, *52*, 3704.
(24) Huang, J. J.; Jiang, Z. Y. *Electrochim. Acta* **2008**, *53*, 7756.
(25) Jiang, X. C.; Herricks, T.; Xia, Y. N. *Adv. Mater.* **2003**, *15*, 1205.
(26) Wang, P.; Xie, T. F.; Li, H. Y.; Peng, L.; Zhang, Y.; Wu, T. S.; Pang, S.; Zhao, Y. F.; Wang, D. J. *Chem.—Eur. J.* **2009**, *15*, 4366.
(27) Huang, S.; Wen, Z.; Zhu, X.; Gu, Z. *Electrochem. Commun.* **2004**, *6*, 1093.
(28) Jiang, C. H.; Zhou, Y.; Honma, I.; Kudo, T.; Zhou, H. S. *J. Power Sources* **2007**, *166*, 514.
(29) Li, Y.; Pan, G. L.; Liu, J. W.; Gao, X. P. *J. Electrochem. Soc.* **2009**, *156*, A495.
(30) Scharner, S.; Weppner, W.; Schmid-Beurmann, P. *J. Electrochem. Soc.* **1999**, *146*, 857.
(31) Li, J. R.; Tang, Z. L.; Zhang, Z. T. *Electrochem. Commun.* **2005**, *7*, 894.